Korean J. Chem. Eng., 32(7), 1249-1257 (2015)
DOI: 10.1007/s11814-014-0354-2

pISSN: 0256-1115
eISSN: 1975-7220

Effects of membrane characteristics on performances of pressure retarded osmosis power system

Sung Soo Hong*, Won Ryoo*, Myung-Suk Chun, and Gui-Yung Chung*,†**

*Department of Chemical Engineering, Hong-Ik University, Mapo-gu, Seoul 121-791, Korea
**Complex Fluids Laboratory, National Agenda Res. Division, Korea Institute of Science and Technology (KIST), Seongbuk-gu, Seoul 136-791, Korea
(*Received 19 March 2014 • accepted 1 December 2014*)

Abstract−Effects of the characteristics of membrane such as water permeability-coefficient, solute permeability-coefficient, and membrane resistivity on the performances of the spiral wound module in the PRO system have been studied numerically. Fluxes of water and solute through membrane, and concentrations and flow rates in the channels were obtained. The water flux through membrane increases almost linearly with the water permeability-coefficient, but it is insensitive to the solute permeability-coefficient. Decreasing the membrane resistivity makes the water flux through membrane and the power density increase. Effects of the membrane resistivity on the water flux through membrane and flow rates in the channels are small when the difference between the inlet-pressures of draw- and feed-channel is large and vice versa. The power density increases and then decreases as the channel-inlet pressure difference increases. The maximum power density is 16 W/m^2 at 14 atm of the channel-inlet pressure difference in our system.

Keywords: Pressure Retarded Osmosis (PRO), Water Permeability Coefficient, Solute Permeability Coefficient, Membrane Resistivity, Water Flux, Power Density

INTRODUCTION

Fossil fuels are being exhausted rapidly because of global population growth and industrial development. Since using fossil fuel has bad influences on the environment, a solution has been sought to replace fossil fuel with renewable energy sources like wind, solar, ocean, and hydraulic power. One renewable energy is salinity power, which can be obtained from the ocean [1-3]. It can be exploited from the entropy of mixing fresh water and seawater, which have different salinities [4], and explained by two basic principles: osmosis [1-3,5] and electro-dialysis [6,7]. The membrane process using osmosis is operated in two ways as forward osmosis (FO) and pressure retarded osmosis (PRO). In the PRO system, the operating pressure is 11-15 bar, which is less than that in the FO system.

When fresh water passes through a channel, part of it permeates through the membrane into the seawater-channel by osmosis due to the concentration differences across membrane [8]. The permeated water raises the pressure in the seawater-channel, and the pressurized seawater comes out through the central tube as brackish water. Power can be obtained from the pressurized seawater. Part of the pressurized seawater recycles to the pressure exchanger to pressurize the seawater-channel where the typical operating pressure is 11-15 bar, which is less than the seawater osmotic pressure, 35 bar. So the system is named the PRO system.

The PRO has been studied since Pattle et al. [9] did researches on harvesting energy using a salinity gradient in 1950's. The concept of PRO was established by Loeb in 1975 [10]. After about two decades, Gerstandt et al. [11] studied the membrane processes for an osmotic power plant and Statkraft company in Norway did research on the PRO to generate power in 1997 [12].

The key point in operating the PRO system is to tailor the membrane structure on which the significant portion of efforts to improve the PRO conditions by decreasing the internal concentration polarizations has been concentrated. Yip et al. [5] and Achilli et al. [13] studied fluxes of water and solute through membrane, including concentration polarizations which affect these fluxes in the PRO system. They also calculated power density accounting for the pressure from the calculated water flux. Similarly, Sundramoorthy et al. [14] carried out an analytical one-dimensional model for the reverse osmosis (RO) system with a spiral wound module. In our previous study, the PRO spiral wound module was studied by two-dimensional modeling where streams of seawater and fresh water were cross-flows. The water flux and the solute flux across membrane were calculated. In addition, changes in concentration, flow rate, and pressure of channel-fluids were obtained [15]. The effects of the inlet-pressure differences between feed-channel and draw-channel were also studied [16].

The main characteristics of membrane which affect the membrane performance are the water permeability-coefficient (A), the solute permeability-coefficient (B), and the membrane resistivity (K). So, effects of the characteristics of membrane on the performances of the PRO power system were studied in a two-dimensional cross-flow system.

THEORETICAL

The spiral wound module is the most common type (Fig. 1) [8,

†To whom correspondence should be addressed.
E-mail: gychung@hongik.ac.kr

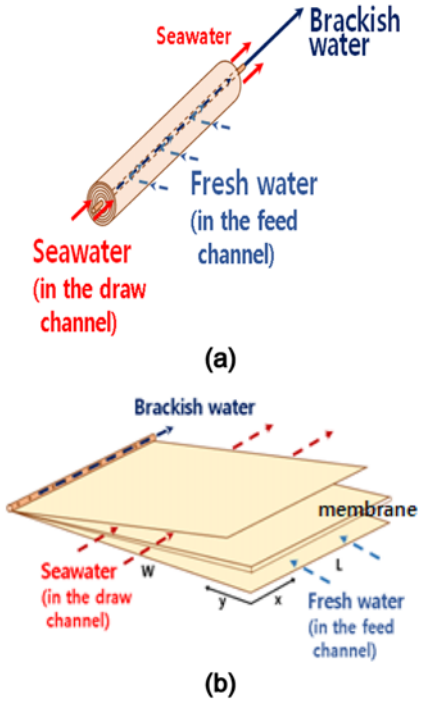

Fig. 1. (a) The schematic diagram of the PRO system. (b) The diagram of the unfolded system. Fresh water flows in the circular direction and gets out through the central tube. On the other hand, seawater flows parallel to the center axis of the central tube.

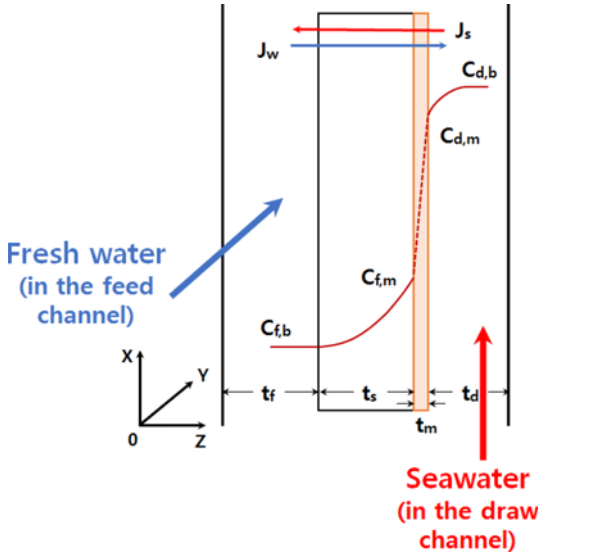

Fig. 2. The distribution of solute (salt) concentration in the system. The subscripts d, f, m, and b mean draw-channel, feed-channel, membrane, and bulk fluid, respectively. J_w and J_s are the water flux and the solute flux through membrane, respectively. F_f and F_d are the flow rates through the feed-channel and the draw-channel, respectively.

17,18]. There is a draw-channel, a membrane and a feed-channel. As mentioned, the PRO system uses osmotic pressure between fresh water and seawater. The fresh water in the feed-channel flows in the circular direction around the central tube. On the other hand, the draw solution, seawater, in the draw-channel flows in the axial direction of the module. While two solutions flow in each channel, part of the fresh water in the feed-channel, circulating around the central tube, permeates through the membrane in the radial direction of the module, mixes with the seawater in the draw-channel, and flows along the axial direction of the module. The rest of the fresh water flows continuously and is collected in the perforated central tube. Then it flows in the axial direction of the tube and leaves the module [19].

The water and the solute (salt) permeate through the membrane due to the osmotic pressure corresponding to the concentration difference. Seawater in the draw-channel gets pressure because of the fresh water penetrating through the membrane. Power is obtained from the increased pressure of the seawater. According to the van't Hoff equation, the osmotic pressure (π) is proportional to the concentration difference between that in the draw-channel and the feed-channel [20]. At 20 °C for a 35 g/*l* salt solution, i.e., seawater, the theoretical osmotic pressure is 29 bar. Once water penetrates through the membrane, the water flux through membrane caused by the osmotic pressure difference has decreased. This is because salt has deposited on the surfaces of the membrane and the support layer.

The distribution of salt concentration is shown in Fig. 2. The z-directional water flux (J_w) through membrane is from the feed- to the draw-channel. On the other hand, the z-directional solute flux (J_s) is the reverse. The general equation of water flux is expressed as follows [21].

$$J_w = A(\Delta\pi_m - \Delta P_m) \quad (1)$$

Here, A [m/(atm·s)] is the water permeability-coefficient across membrane. $\Delta\pi_m$ [atm] and ΔP_m [atm] are the osmotic pressure difference and the local pressure difference across the membrane, respectively. McCutcheon et al. [22] modeled the water flux in the forward osmosis (FO).

Although the membrane rejects the majority of salt, a small amount permeates through membrane into the water-channel because of the concentration gradient. The solute flux is expressed as follows [23]:

$$J_s = -B(C_{d,m} - C_{f,m}) \quad (2)$$

Here, B [m/s] is the solute permeability-coefficient. $C_{d,m}$ and $C_{f,m}$ are concentrations on the membrane surfaces at the draw- and the feed-channel sides, respectively.

In the PRO system, the concentration polarization due to an increased osmotic pressure at the membrane active layer surface is detrimental to the water flux as shown in Fig. 2 [24]. There are two concentration polarizations: the internal concentration polarization (ICP) within the membrane, and the external concentration polarization (ECP) on the outside surfaces of membrane. They can be significant for the high performance of the PRO membrane which should have small membrane structural parameters and large water fluxes [25]. The membrane in the PRO system should have a large water permeability-coefficient (A) and a small solute permeability-coefficient (B) in order to obtain more power. In addition, the inner structure of the membrane must not allow salt to

accumulate inside the membrane significantly.

Yip et al. [5] obtained the water flux (J_w) and the solute flux (J_s) through membrane including those two concentration polarizations. J_w in Eq. (1) is expressed as follows:

$$J_w = A\left[\frac{\pi_d \exp\left(-\frac{J_w}{k}\right) - \pi_f \exp\left(\frac{J_w S}{D}\right)}{1+\frac{B}{J_w}\left\{\exp\left(\frac{J_w S}{D}\right) - \exp\left(-\frac{J_w}{k}\right)\right\}} - \Delta P_m\right] = A\left[\frac{\pi_d \exp\left(-\frac{J_w}{k}\right) - \pi_f \exp(J_w K)}{1+\frac{B}{J_w}\left\{\exp(J_w K) - \exp\left(-\frac{J_w}{k}\right)\right\}} - \Delta P_m\right] \quad (3)$$

Here, subscripts d, f, and m stand for draw-channel, feed-channel, and membrane, respectively. ΔP_m is the local pressure difference across the membrane. k [m/s] is the mass transfer coefficient, D [m^2/s] the bulk diffusion coefficient of solute, and S (=$t_s \cdot \tau/\varepsilon$) [m] the structure parameter of membrane; t_s, τ, and ε are thickness, tortuosity, and porosity of the support layer, respectively. The ratio of S to D (S/D) is the membrane resistivity (K). So J_w can be also expressed as a function including K as shown in Eq. (3). The membrane in a module must have a design that reduces the thickness of the support layer to a minimum [10].

The solute flux through membrane (J_s) in Eq. (2) including concentrations across membrane (C_d and C_f) is expressed as follows.

$$J_s = -B\left[\frac{C_d \exp\left(-\frac{J_w}{k}\right) - C_f \exp\left(\frac{J_w S}{D}\right)}{1+\frac{B}{J_w}\left\{\exp\left(\frac{J_w S}{D}\right) - \exp\left(-\frac{J_w}{k}\right)\right\}}\right] \quad (4)$$

In the PRO system, power is generated with the hydraulic pressure of the draw fluid increased by the water flux from the feed-channel through membrane. The power density (P_D) is obtained by multiplying the water flux through membrane and the pressure difference between the draw-channel and the feed-channel (ΔP_m) [5].

$$P_D = J_w \Delta P_m \quad (5)$$

The transport properties such as the coefficients of water permeability (A) and solute permeability (B) of the PRO membrane can be determined experimentally [4,5]. The water permeability-coefficient (A) is determined by measuring how much water permeates through membrane at an applied hydraulic pressure. The solute permeability-coefficient (B) is also measured experimentally in a similar way [26]. The membrane resistivity (K) is calculated with the diffusion coefficient and values of thickness, porosity and tortuosity of the membrane. These values in our study were taken from the references.

MODEL DEVELOPMENT

A schematic diagram of the system for the modeling is shown in Fig. 3. The length and the width of membrane are L and W, respectively. In each channel, fresh water in the feed-channel flows in the y-direction and seawater in the draw-channel flows parallel to the axis of the tube in the x-direction. There are fluxes of water (J_w) and solute (J_s) in the z-direction through pores in the membrane as in Fig. 2. Here, J_w has a positive value and J_s has a negative one. Fresh water in the feed-channel and seawater in the draw-channel are cross-flows. In the module, the membrane which consists of a thin active layer supported by a thick layer of porous polymer and fabric support is wound around the central tube. The membrane studied in this research was made of polyamide and its characteristic values are in Table 1. In each channel, z-directional changes of pressure, concentration, and velocity were neglected. They change only in x- and y-directions. In addition, diffusion in channels was assumed negligible compared with convection.

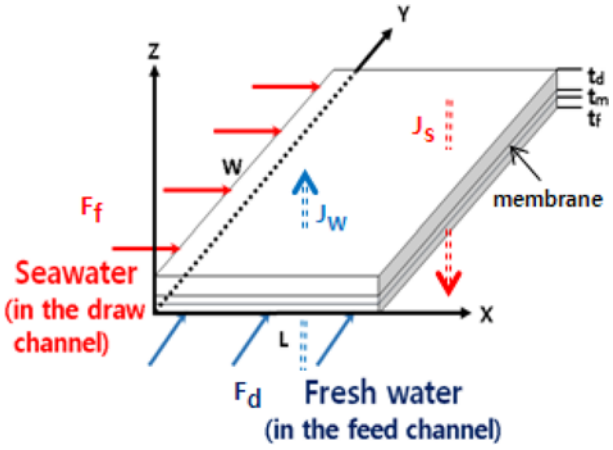

Fig. 3. The schematic diagram of the system for the modeling. L is the length of cylindrical membrane and W is the width of the unfolded membrane. t_d, t_m, and t_f are thicknesses of the draw-channel, the membrane, and the feed-channel.

Table 1. Characteristic values of the PRO system used in the modeling

Dimensions	Values
Length of the membrane, L [m]	1
Width of the membrane, W [m]	8.4
Thickness of the membrane, t_m [m]	4×10^{-5}
Thickness of the feed channel, t_f [m]	8×10^{-4}
Thickness of the draw channel, t_d [m]	5×10^{-4}

The total mass balance and the mass balance of salt in the draw- and the feed-channels including the water flux through membrane are as follows:

$$\frac{dF_d}{dx} = WJ_w \qquad \text{b.c. at x=0 \& all y, } F_d = F_{d0} \quad (6)$$

$$\frac{dF_f}{dy} = -LJ_w \qquad \text{b.c. at y=0 \& all x, } F_f = F_{f0} \quad (7)$$

Since the water flux through a membrane is a positive value, it increases the draw-flow rate in Eq. (6) and decreases the feed-flow

Table 2. Parameter values of the PRO system used in the modeling [13,28,29]

Parameters	Values
Water permeability-coefficient, A_o [m/(atm·s)]	9.5×10^{-7}
Salt permeability-coefficient, B_o [m/s]	8.5×10^{-10}
Structural parameter of the membrane, $S=t_s\tau/\varepsilon$ [m]	3.5×10^{-4}
Diffusion coefficient of salt, D [m^2/s]	1.5×10^{-9}
Membrane resistivity, K_o (=S/D) [s/m]	2.3×10^{5}
Mass transfer coefficient of salt, k [m/s]	8.5×10^{-5}
Friction parameter in the channels, b [atm·s/m^4]	8500
Inlet flow rate of the feed-flow, F_{f0} [m^3/s]	1.0×10^{-3}
Inlet flow rate of the draw-flow, F_{d0} [m^3/s]	1.0×10^{-3}
Inlet pressure of the draw-flow, P_{d0} [atm]	29

rate in Eq. (7). The pressure drop in the draw-channel is proportional to the flow rate by Darcy law [27] as follows:

$$\frac{dP_d}{dx} = -bF_d \qquad \text{b.c. at x=0 \& all y, } P_d=P_{d0} \qquad (8)$$

Here, b (atm·s·m^{-4}) is the friction parameter [28]. The pressure drop in the feed-channel can be also expressed in a similar way.

Parameter values used in the modelling (Table 2) were taken from the references [13,28,29]. Calculations were by the finite difference method. The length, L, in x-direction and the width, W, in y-direction were divided into 20 and 40 elements, respectively. The water flux was calculated with Eq. (3) at first. Then the solute flux was calculated with the calculated value of water flux. Concentrations, flow rates, and pressures in the channels were calculated. The power density was also calculated. When parameter values were changed, the expected changes of performance were estimated. In addition, trends and reasons for the changes have been explained.

RESULTS AND DISCUSSION

Characteristic values of the membrane affect the performance of the PRO system. In this research, effects of the water permeability-coefficient (A), the solute permeability-coefficient (B), and the membrane resistivity (K) on the performances of the spiral wound module in the PRO system have been studied numerically. The fluxes of water and solute through the membrane were calculated. Furthermore, changes and distributions of concentrations and volumetric flow rates in the channels were obtained. Power density was also evaluated.

1. Effects of Water Permeability-coefficient

The water flux through membrane (J_w) depends on the water permeability-coefficient (A) as in Eq. (3). In addition, the solute flux through membrane (J_s) also depends on A, since J_w is included in the equation of J_s as in Eq. (4). Changes of J_w and J_s with A are shown in Fig. 4. Both J_w and J_s were calculated at the channel-inlet concentration difference of 35 g NaCl/L and the channel-inlet pressure difference (ΔP_{mo}) of 1 atm. Here, the channel-inlet differences mean differences between those at the feed- and the draw-channel entrances. The reference value of the water permeability-coefficient, A_0, is 9.5×10^{-7} [m/atm·s]. It is natural that a large value of A

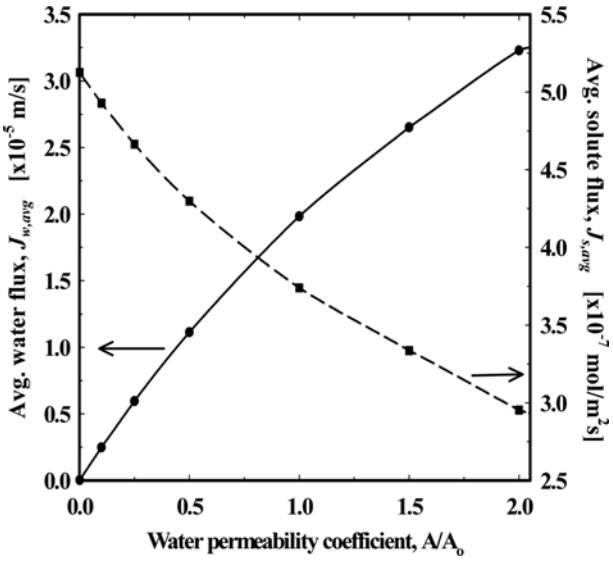

Fig. 4. The average water flux ($J_{w,avg}$) and the average solute flux ($J_{s,avg}$) through membrane versus the dimensionless water permeability-coefficient (A/A_o) at $A_o=9.5\times10^{-7}$ m/atm·s.

gives a large value of J_w as in Eq. (3). J_w increases almost linearly with A. In our system, the areal average of J_w is 2×10^{-5} m/s at A_o and it increases 63% at $2A_o$.

On the contrary, J_s driven by the concentration difference across the membrane decreases with A, because the direction of J_s is opposite to that of J_w. So the solute transfer is hindered by the large opposite-directional water flux. It can be also explained in another way. The increase of water permeability (A) increases the water flux through membrane. This increased water flux causes to decrease the difference between concentrations at both sides of membrane. Because the concentration difference is decreased, the solute flux becomes small.

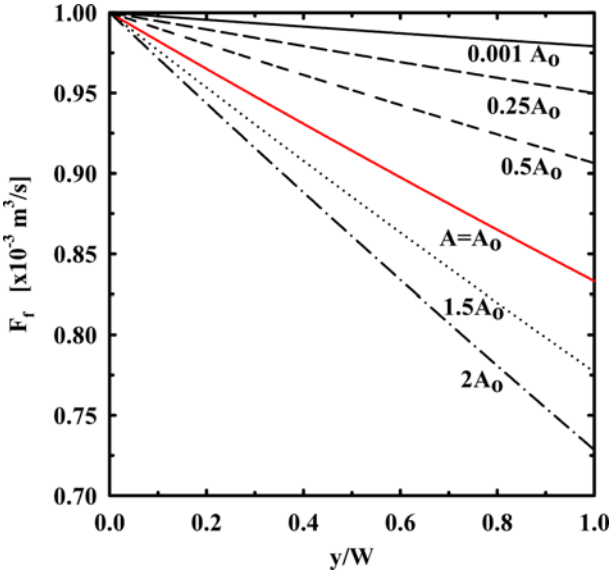

Fig. 5. Changes of the flow rate in the feed-channel along the direction of flow at different water permeability-coefficients of the membrane at $A_o=9.5\times10^{-7}$ m/atm·s.

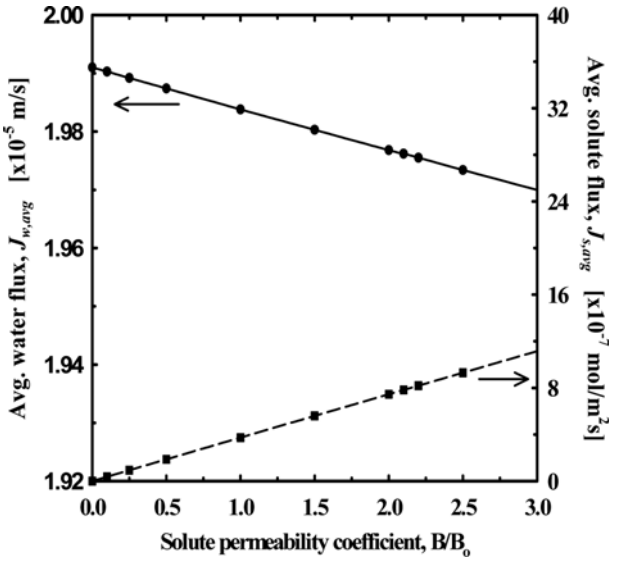

Fig. 6. The average water flux ($J_{w,avg}$) and the average solute flux ($J_{s,avg}$) through membrane versus the dimensionless solute permeability-coefficient (B/B_o) at $B_o=8.5\times10^{-10}$ m/s.

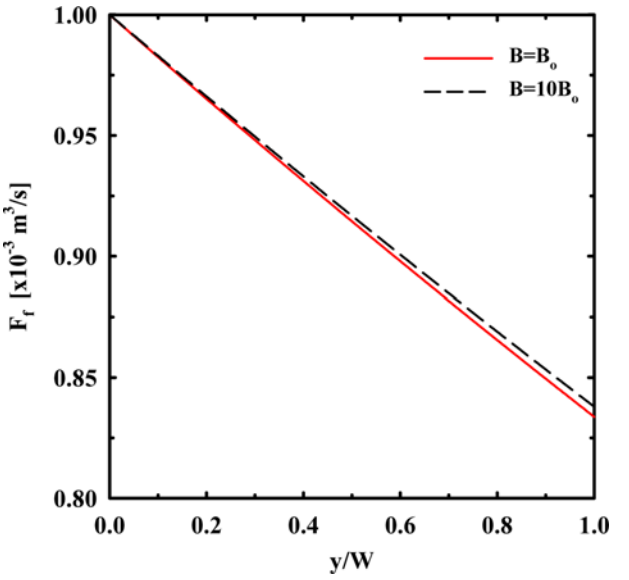

Fig. 7. Changes of the flow rate in the feed-channel along the direction of flow at different solute permeability-coefficients of the membrane at $B_o=8.5\times10^{-10}$ m/s.

The volumetric flow rate of water in the feed-channel (F_f) decreases along the direction of fluid, since part of water (J_w) penetrates into the membrane. Changes of F_f along the y-direction at different values of A are shown in Fig. 5. As expected from the large J_w at a large A, the flow rate in the feed channel (F_f) decreases about 17% at A_o and about 27% at $2A_o$ in our system while the fluid passes through the channel. At the same time, the flow rate of seawater in the draw-channel (F_d) increases almost the same amount as the decreased amount of F_f while the fluid passes through the channel.

2. Effects of Solute Permeability-coefficient

The solute permeability-coefficient (B) affects mainly J_s as in Eq. (4). Changes of J_w and J_s at different values of B are shown in Fig. 6. Calculations were done at B_o (i.e., 8.5×10^{-10} m/s) and 35 g NaCl/l of the channel-inlet concentration difference. As B increases, J_s increases and J_w decreases. The increase of B makes J_s increase as in Eq. (4). However, it decreases the osmotic pressure difference corresponding to the concentration polarization. Hence, it makes J_w decrease a little.

J_w is not sensitive to B as in Fig. 6 compared with A as in Fig. 4. J_w increases 63% when the value of A changes from A_o to $2A_o$ in Fig. 4. However, it decreases only 0.3% when the value of B changes from B_o to $2B_o$. On the other hand, J_s is affected deeply by both A and B. It decreases about 21% when A is doubled, and increases 90% when B is doubled in our system.

The flow rates in the channels (F_f and F_d) are affected more by J_w than by J_s. Hence, as J_w is insensitive to B, it can be expected that the flow rates in channels will not change much due to the size of B. In Fig. 7, the flow rate in the feed-channel (F_f) decreases about 16.8% at B_o and about 16.2% at $10B_o$ in our system while the fluid passes through the channel. The difference between the decreased amounts of F_f at B_o and $10B_o$ is very small (0.6%) as expected. Even though the difference is very small, the flow rate in the feed-channel at $10B_o$ decreases less than that at B_o due to a small J_w at $10B_o$ while the fluid passes through the channel.

3. Effects of Membrane Resistivity

The ratio of S to D (S/D) is defined as the membrane resistivity (K). Here, S [m] is the structure parameter and D [m^2/s] is the bulk diffusion coefficient. The structure parameter S ($=t_s\tau/\varepsilon$) involves support layer's thickness (t_s), tortuosity (τ), and porosity (ε). These values have an effect on J_w in Eq. (3), J_s in Eq. (4) and the distributions of concentrations and flow rates in the channels. The areal average water fluxes through membrane ($J_{w,avg}$) vs. the channel-inlet pressure difference (ΔP_{mo}) at different values of membrane resistivity are shown in Fig. 8. The reference value of the membrane resis-

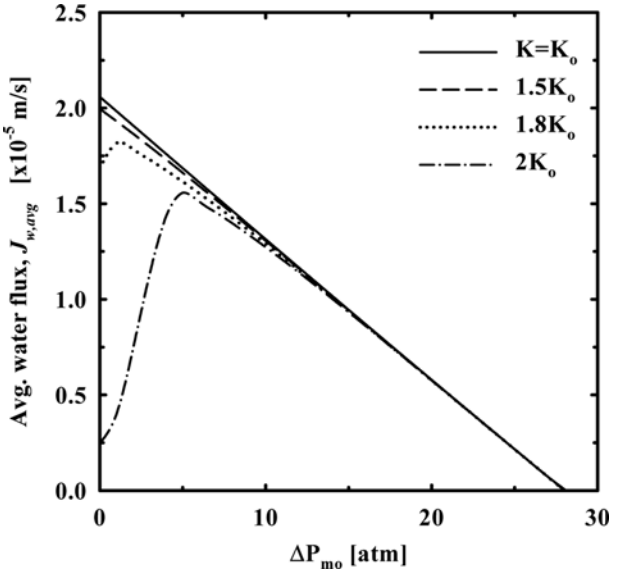

Fig. 8. The average water flux through membrane ($J_{w,avg}$) versus the inlet pressure difference (ΔP_{mo}) at different values of membrane resistivity at $K_o=2.3\times10^5$ s/m and $\Delta C_o=35$ g/L.

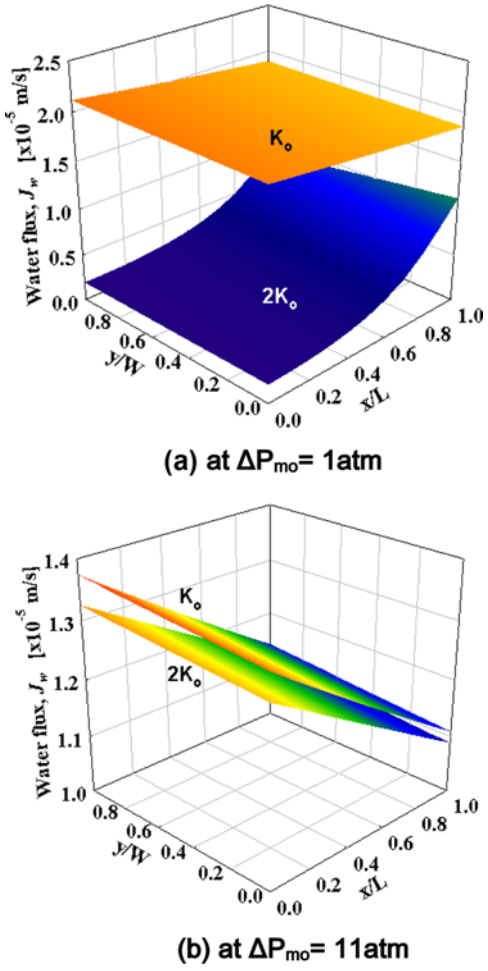

Fig. 9. Distributions of the water flux through membrane (J_w) at two different values of membrane resistivity of K_o and $2K_o$ at K_o= 2.3×10^5 s/m.

tivity (K_o) is 2.3×10^5 s/m. The concentration polarization in the PRO system is related to the membrane resistivity. So the increase of the membrane resistivity causes a decrease of osmotic pressure, and, as a result, the decrease of J_w as in Fig. 8. When ΔP_{mo} is small, the effect of the membrane resistivity on J_w is clearly seen. On the other hand, when ΔP_{mo} is greater than 5 atm, it is very small.

Seawater in the draw-channel flows in the x-direction and fresh water in the feed-channel flows in the y-direction. They are cross-flows in our spiral wound module. Distributions of J_w at two values of membrane resistivity (K_o and $2K_o$) are shown in Fig. 9. When thickness and tortuosity of membrane are large and porosity of membrane is small, membrane resistivity is large. So J_w is small at a large membrane resistivity. Therefore the contour plane of J_w at $2K_o$ is under that at K_o in Fig. 9. Furthermore, the change of J_w along the direction of fresh water (y-direction) is very small. But, that along the direction of seawater (x-direction) is large at both K_o and $2K_o$ in Fig. 9.

The increase of concentration of solute in the feed-channel is due to the inflow of J_s. But the concentration in the feed-channel is very low. So the effect of J_s on the increase of concentration in the feed-channel is small. On the other hand, the decrease of concentration of solute in the draw- channel is due to the inflow of J_w. So the decrease of the concentration of solute in the draw-channel is large. Since J_w is due to the difference of the concentrations in the draw- and the feed-channel, it is affected more by the change of concentration in the draw-channel rather than by that in the feed-channel. So J_w in Fig. 9 changes more along the direction of seawater (x-direction).

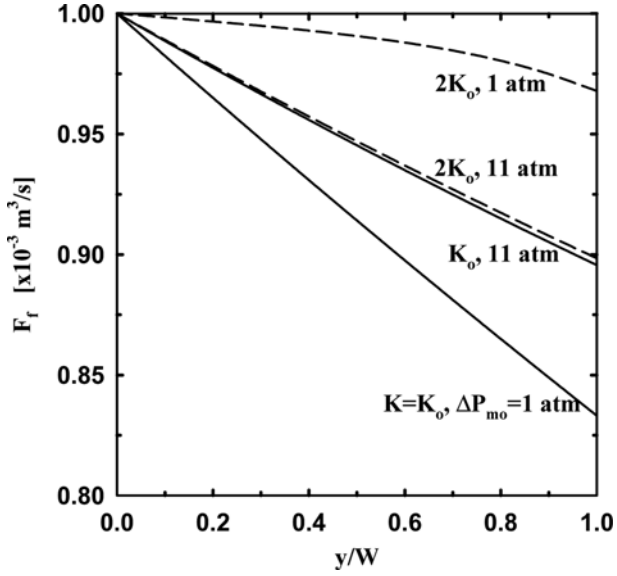

Fig. 10. Changes of the feed-channel flow rate along the direction of flow at two different inlet-pressure differences and two different values of membrane resistivity in the feed-channel at K_o=2.3×10^5 s/m.

At 1 atm of ΔP_{mo} in Fig. 9(a), J_w at $2K_o$ is much less than that at K_o. However, at 11 atm of ΔP_{mo} in Fig. 9(b), J_w at $2K_o$ is about 3% less than that at K_o. This is because the increase of J_w due to an increase of ΔP_{mo} is bigger than that due to a decrease of K. In other words, J_w is big already at a large ΔP_{mo}. So the increase of J_w due to a decrease of K is a small portion of the whole J_w. As a result, the effect of membrane resistivity on J_w appears small at a large ΔP_{mo}.

The flow rate in the feed-channel (F_f) decreases due to the outflow of J_w. So K and ΔP_{mo} affects F_f in the same way as how they affects J_w. The membrane resistivity affects F_f little at a large ΔP_{mo}, since the effect of large ΔP_{mo} on J_w is big already. This can be confirmed by observing the changes of F_f along the direction of flow at different values of K and ΔP_{mo} in Fig. 10. At a small ΔP_{mo} of 1 atm, F_f decreases about 17% at K_o and about 3% at $2K_o$ in our system while the fluid passes through the channel. However, at a large ΔP_{mo} of 11 atm, F_f decreases about 11% at K_o and 10% at $2K_o$ in our system while the fluid passes through the channel. There is no big difference between F_f's at K_o and $2K_o$ when ΔP_{mo} is large. So it can be concluded that effect of K on F_f is large at a small ΔP_{mo} and vice versa.

The difference of concentrations in the feed- and the draw-channel induces J_w. In addition, the difference between concentrations in channels becomes smaller quickly at a small K, since J_w is large. As a result, J_w and, as a result, F_f decrease along the direction of flow quickly at a small K. So it is confirmed again that effects of K on the flow rates in channels are large at a small ΔP_{mo}.

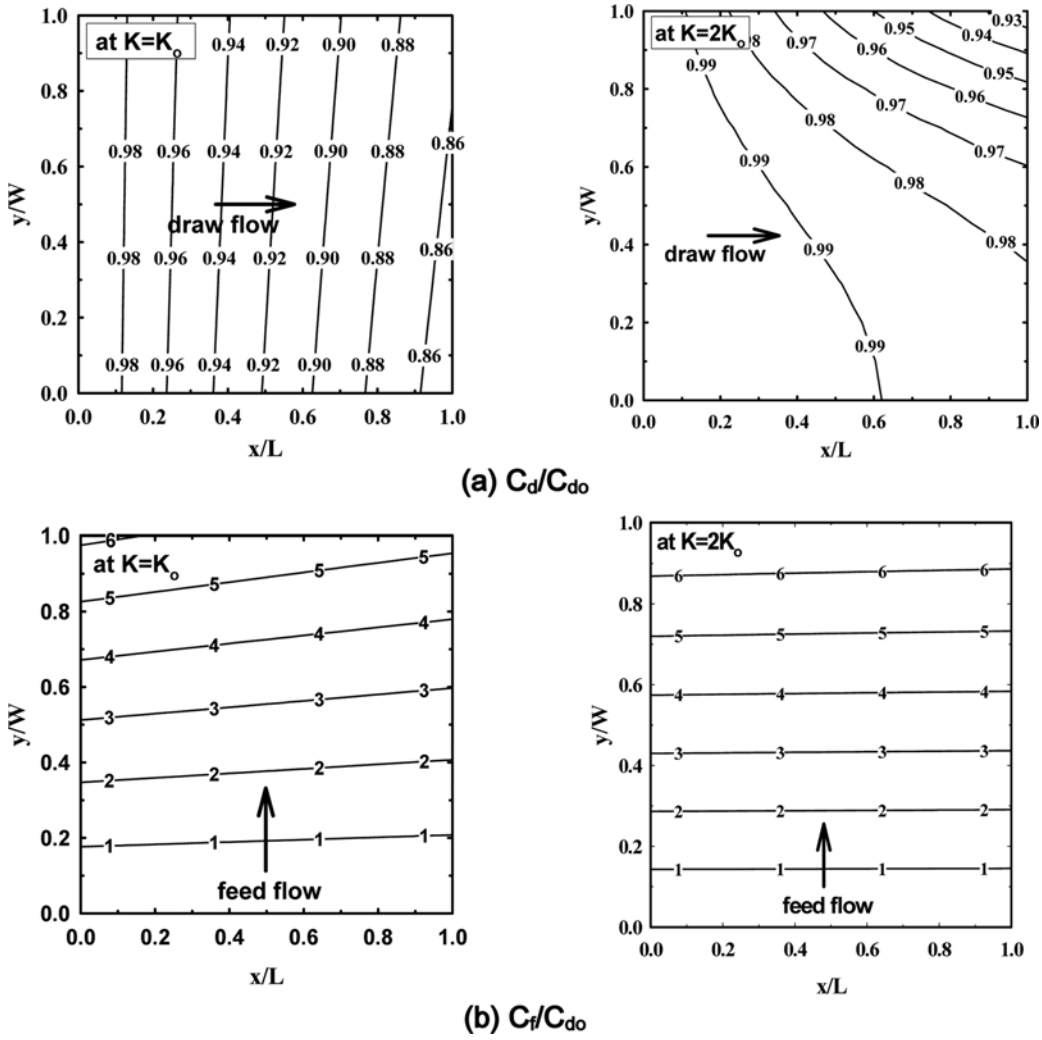

Fig. 11. Distributions of the dimensionless concentration (C/C_{do}) (a) in the feed-flow and (b) in the draw-flow at ΔC_o=35 g/L and ΔP_{mo}= 1 atm.

The concentration of solute (salt) in the draw-fluid decreases along the direction of fluid because of the inflow of J_w as shown in Fig. 11(a). It decreases 14% at K_o and 5% at $2K_o$ in our system while the draw-fluid passes through the channel. Since J_w is large at a small K, the concentration of solute at K_o decreases more than that at $2K_o$ does. However, the concentration of solute in the feed-fluid increases slightly along the direction of fluid due to the inflow of J_s as shown in Fig. 11(b). Here, the effect of the membrane resistivity is small.

4. Power Density

In the PRO system, power is generated with the hydraulic pressure of the draw fluid increased by the water flux from the feed-channel through membrane. The power density (P_D) in Eq. (5) is obtained by multiplying J_w and the difference between pressures in the draw-channel and the feed-channel (ΔP_m). Here, J_w is dependent on the local ΔP_m as shown in Eq (3). Furthermore, ΔP_m depends on ΔP_{mo} (ΔP_m at the channel-inlet). So it can be said that J_w and P_D are dependent on ΔP_{mo}. The water flux through membrane and the power density vs. the difference between the inlet-pressures of channels (ΔP_{mo}) at K_o and $2K_o$ are shown in Fig. 12. J_w at K_o decreases continuously as ΔP_{mo} increases. On the other hand, J_w

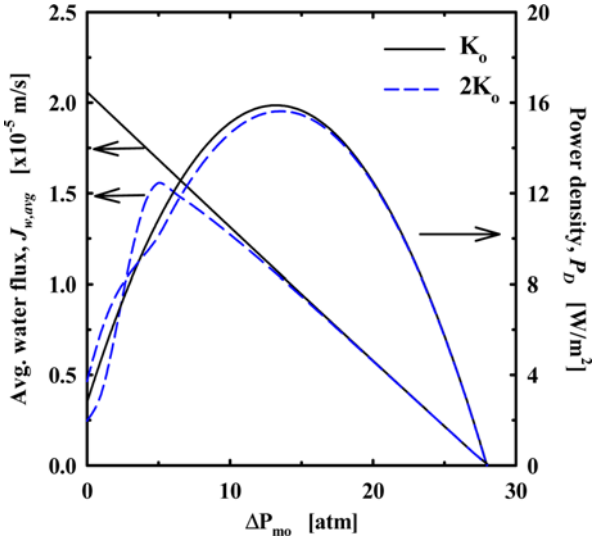

Fig. 12. The average water flux through membrane ($J_{w,avg}$) and the power density (P_D) versus the inlet-pressure difference (ΔP_{mo}) at ΔC_o=35 g/L.

at $2K_o$ increases at first and then decreases. Effects of K on J_w in Fig. 12 were explained already in Fig. 8. In addition, P_D increases at first because of the increasing ΔP_m, and decreases later because of the decreasing J_w at both K_o and $2K_o$. The maximum power density is 16 W/m^2 at 14 atm of the channel-inlet pressure difference in our system.

If J_w is small, the variation of ΔP_m is small. So the areal average of ΔP_m at $2K_o$ is a little larger than that at K_o. As a result, P_D at $2K_o$, which is the multiplication of J_w and a little larger ΔP_m, appears a little bigger than P_D at K_o as shown in Fig. 12. However, when ΔP_{mo} is larger than 5 atm, J_w at $2K_o$ is a little smaller than that at K_o. Then the variation of ΔP_m at $2K_o$ is a little smaller than that at K_o. In other words, the areal average of ΔP_m at $2K_o$ is similar to that at K_o. So, as shown in Fig. 12, P_D at $2K_o$ is a little smaller than that at K_o. It can be concluded that the effect of K on P_D is small when ΔP_{mo} is large.

CONCLUSIONS

Characteristic values of the membrane are important for the good performance of the PRO system. Effects of the water permeability-coefficient, the solute permeability-coefficient, and the membrane resistivity were studied in the two-dimensional mathematical modeling.

The water flux through a membrane increases almost linearly with the water permeability coefficient (A). On the other hand, the solute flux decreases with A. When the value of A becomes twice, J_w increases 63% more and the flow rate in the feed-channel decreases about 59% more in our system while the fluid passes through the channel.

The solute permeability-coefficient (B) affects mainly J_s. As B increases, J_s increases and J_w decreases. However, J_w is insensitive to B compared with A. As a result, the flow rates in channels are also insensitive to B.

Decreasing the membrane resistivity (K) makes J_w and the power density (P_D) increase. But the increase of J_w due to the decrease of K is a small portion of the whole J_w. So effects of K on J_w and the flow rates in the channels (F_f and F_d) are small when ΔP_{mo} is large and vice versa.

The concentration of solute in the draw-fluid decreases 14% at K_o and 5% at $2K_o$ in our system while the fluid passes through the channel. However, the effect of K on the concentration of solute in the feed-fluid is small. P_D increases at first because of the increasing ΔP_m, and decreases later because of the decreasing J_w at both K_o and $2K_o$. The maximum power density is 16 W/m^2 at 14 atm of the channel-inlet pressure difference in our system. When ΔP_{mo} is small, P_D is a little large at a large K. However, when ΔP_{mo} is large, the effect of K on P_D is small.

ACKNOWLEDGEMENT

This work was supported by the New & Renewable Energy Technology Development Program of the Korea Institute of Energy Technology Evaluation and Planning (KETEP) grant funded by the Korea government Ministry of Knowledge Economy (No. 20103020070060). This work was also supported by the 2015 Hongik University Research Fund.

NOMENCLATURE

A : solvent (i.e., water) permeability-coefficient [m/atm·s]
B : ssolute (i.e., salt) permeability-coefficient [m/s]
b : friction parameter [atm·s/m^4]
C_d, C_f : concentrations of salt in the channels [kg/m^3]
D : diffusion coefficient in the porous support layer [m^2/s]
F_d, F_f : volumetric flow rates in the channels [m^3/s]
J_w : water flux [m/s]
J_s : solute flux [mol/m^{2}s]
k : mass transfer coefficient of solute [m/s]
L : x-directional length in the feed channel [m]
P_d, P_f, P_m : pressures in the channels and on the membrane [atm]
P_D : power density [W/m^2]
R : gas constant (=0.082) [atm·m^3/(mol·K)]
S (=$t_s\tau/\varepsilon$) : structure parameter of the support layer [m]
t_d, t_f : thicknesses of the channels [m]
t_m : thickness of the membrane [m]
W : y-directional width in the draw-channel [m]
x : x-directional distance along the flow in the draw-channel [m]
y : y-directional distance along the flow in the feed-channel [m]

Greek Letters

Δ : difference between the draw-channel and the feed-channel
ε : porosity of the support layer
τ : tortuosity of pores in the support layer

Subscripts

d : draw-channel
f : feed-channel
m : membrane
o : at the inlet of the channel
s : solute (salt)
w : solvent (water)

REFERENCES

1. A. T. Jones and W. Rowley, *Mater. Technol. Soc. J.*, **36**, 85 (2003).
2. N. Y. Yip and M. Elimelech, *Environ. Sci. Technol.*, **46**, 5230 (2011).
3. N. Y. Yip and M. Elimelech, *Environ. Sci. Technol.*, **45**, 10273 (2011).
4. T. Thorsen and T. Holt, *J. Membr. Sci.*, **335**, 103 (2009).
5. N. Y. Yip, A. Tiraferri, W. A. Phillip, J. D. Schiffman, L. A. Hoover, Y. C. Kim and M. Elimelech, *Environ. Sci. Technol.*, **45**, 4360 (2011).
6. K. S. Kim, W. Ryoo, M. S. Chun, G. Y. Chung and S. O. Lee, *Korean J. Chem. Eng.*, **29**, 162 (2012).
7. K. S. Kim, W. Ryoo, M. S. Chun and G. Y. Chung, *Desalination*, **318**, 79 (2013).
8. I. L. Alsvik and M.-B. Hägg, *Polymers*, **5**, 303 (2013).
9. R. E. Pattle, *Nature*, **174**, 660 (1954).
10. A. Achilli and A. E. Childress, *Desalination*, **261**, 205 (2010).
11. K. Gerstandt, K. V. Peinemann, S. E. Skilhagen, T. Thorsen and T. Holt, *Desalination*, **224**, 64 (2008).
12. Statkraft osmotic power prototype plant design, 21. Dec. 2013, (http://www.statkraft.com/energy-sources/osmotic-power/pro-

totype/pant-design.aspx).
13. A. Achilli, T. Y. Cath and A. E. Childress, *J. Membr. Sci.*, **343**, 42 (2009).
14. S. Sundaramoorthy, G. Srinivasan and D. V. R. Murthy, *Desalination*, **280**, 403 (2011).
15. S.-S. Hong, W. Ryoo, M.-S. Chun, S. O. Lee and G.-Y. Chung, *Desalination and Water Treatment*, **52**, 6333 (2014).
16. S.-S. Hong, W. Ryoo, M.-S. Chun and G.-Y. Chung, *Korean Chem. Eng. Res.*, **52**, 68 (2014).
17. T. Y. Cath, A. E. Childress and M. Elimelech, *J. Membr. Sci.*, **281**, 70 (2006).
18. W. A. Phillip, J. S. Yong and M. Elimelech, *Environ. Sci. Technol.*, **44**, 5170 (2010).
19. J. Schwinge, P. R. Neal, D. E. Wiley, D. F. Fletcher and A. G. Fane, *J. Membr. Sci.*, **242**, 129 (2004).
20. S. T. Hwang, *Korean J. Chem. Eng.*, **28**, 1 (2011).
21. K. L. Lee, R. W. Baker and H. K. Lonsdale, *J. Membr. Sci.*, **8**, 141 (1981).
22. J. R. McCutcheon and M. Elimelech, *AIChE J.*, **53**, 1736 (2007).
23. Y. You, S. Huang, Y. Yang, C. Liu, Z. Wu and X. Yu, *Advances in Computer Sci. Eng.*, **141**, 307 (2012).
24. Q. She, X. Jin and C. Y. Tang, *J. Membr. Sci.*, **401**, 262 (2012).
25. S. Kim and E. M. V. Hoek, *Desalination*, **186**, 111 (2005).
26. Y. C. Kim, Y. Kim, D. W. Oh and K. H. Lee, *Environ. Sci. Technol.*, **47**, 2966 (2013).
27. S. Senthilmurugan, A. Ahluwalia and S. K. Gupta, *Desalination*, **173**, 269 (2005).
28. S. Sundaramoorthy, G. Srinivasan and D. V. R. Murthy, *Desalination*, **277**, 257 (2011).
29. L. Y. Hung, S. J. Lue and J. H. You, *Desalination*, **265**, 67 (2011).